

Low Heat Input Welding by Continuous-Wave Nd:YAG Laser Processing #M210

Steve Roy	Kevin J. Ely
Trumpf Laser Systems Inc.	Edison Welding Institute
Farmington, Connecticut, USA	Columbus, Ohio, USA

Abstract

Low-power applications of laser technology include the manufacture of fuel injectors, pacemakers, and electronic assemblies. For many electronic packages, the final sealing operation can expose the heat-sensitive glass-to-metal seals, semiconductors, and any plastics to severe thermal extremes. Traditional methods of hermetically sealing enclosures use pulsed Nd:YAG. Pulsed processing is used with the theory that the high peak pulse energy will allow adequate penetration, and the low average power will keep the total heat input to a minimum. This approach, however, does not always account for the need of 75-80% overlap of the pulses needed to achieve hermeticity. This requirement for overlap fixes the table feedrate and dictates a finite time of laser illumination on the device. Hence, the effective heat input is a strong function of the time of laser illumination, not just average power. In this work, we demonstrate that the total time of laser illumination on the part is critical, and that high brightness continuous-low divergence continuous wave (CW) laser processing can achieve thermal inputs equal to or less than pulsed processes. From this work, it will be shown that 0.25-mm penetration welds can be made in Ti6Al4V at feed-rates of 85 ipm with maximum temperatures below 300°C.

Introduction

Low-power applications of laser technology include the manufacture of fuel injectors, pacemakers, and electronic assemblies. For many electronic packages, the final sealing operation can expose the heat-sensitive glass-to-metal seals, semiconductors, and any plastics to severe thermal extremes. Traditional methods of hermetically sealing enclosures use pulsed Nd:YAG. Pulsed processing is used with the theory that the high peak pulse energy will allow adequate penetration, and the low average power will keep the total heat input to a minimum. This approach, however, does not always account for the need of 75-80% overlap of the pulses needed to achieve hermeticity. This requirement for overlap fixes the table feedrate and dictates a finite time of laser illumination on the device. Hence, the effective heat input is a strong function of the time of laser illumination, not just average power. In this work, we demonstrate that the total time of laser illumination on the part is critical, and that high brightness continuous-wave (CW) laser processing can achieve thermal inputs equal or less than pulsed processes.

In pulsed processes, while the average power can be comparable to most CW processes for any given penetration, the time on the part to complete the weld can be much longer. This is due to the need for successive spot overlap to achieve hermeticity. Typically, a 75-80% overlap is required to achieve hermeticity. This overlap fixes the feedrate of the table for any given pulse frequency. This maximum table speed (for 75% overlap) can be calculated by:

$$\text{table speed (ips)} = \frac{\frac{\text{pulses}}{\text{sec}} \times \text{spot diameter}}{1.75} \times \frac{\text{inches}}{1.75}$$

Hence, in pulsed processing the time of illumination becomes fixed, and is a function of the system's pulse rate and spot size.

New CW Nd:YAG systems have become available which have very good beam quality and power output. Beam quality is a very important parameter that defines the ability of the laser to achieve adequate penetration at any given power. Lasers with high brightness (good beam quality) can generate a smaller focused spot and allow for greater penetration at lower average powers. Using this type of system, it may be possible to achieve a lower total heat input for a given requirement of penetration. The focus of this study was to assess the temperature buildup in typical medical enclosures of 0.75-mm-thick Ti6Al4V using CW ND:YAG laser processing.

Equipment and Materials

The experiment was set up to assess the maximum temperature due to CW laser processing. Bead-on-plate specimens of 0.75-mm-thick Ti6Al4V were used. Strips of Ti plate were cut to approximately 1.5 × 6 in. and Type E thermocouples were welded on the far side. Data was collected by standard multi-channel mV meters. Transverse bead-on-plate CW welds were made across the top surface of each plate. Figure 1 is a sketch of the typical weld sample.

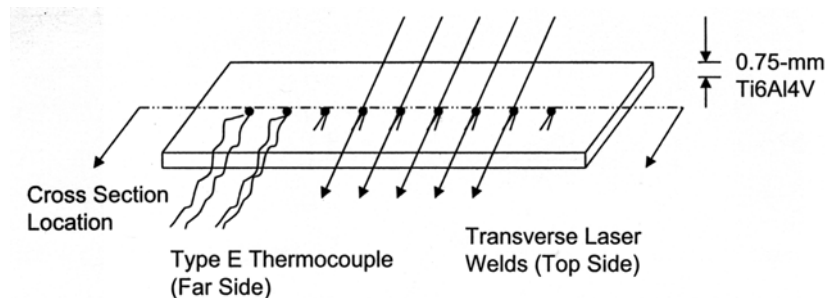


Figure 1. Typical Bead-on-Plate Weld Sample, 0.75-mm Ti6Al4V with Type E Thermocouples (Far Side) and Weld Beads Transverse on the Top Side

All welds were completed using a Trumpf-HAAS 353 Nd:YAG laser in CW mode. The beam was delivered to the workpiece via a stepped index 300- μ m fiber, a 200-mm collimating lens, and either a 200- or 150-mm focal lens. The typical spot size was 0.008-0.012 in. dependent on the focal lens that was used. An AEROTECH U511CNC controller and Aerotech x-y table controlled the table motion and speed. The Type E thermocouples were calibrated to ice water and boiling water before each weld run. The probes were stated to be linear beyond this calibration and minimal error was expected beyond the calibration range up to 500°C.

Experimental Setup and Results

Transverse laser welds were made across the titanium strips using various laser powers, feedrates, and lens combinations. The maximum temperature was recorded via the thermocouples. The test strips were carefully mounted to avoid shorting the thermocouple signal or by providing local heatsinking that would effect the readings. After welding, the strips were cross sectioned down the long axis of the test coupon as shown in Figure 1. From this cross section, the weld penetration was measured.

CW welds were made at various powers and using both focal length lenses. The goal was to achieve a consistent penetration of 0.20-0.25 mm. This penetration is consistent with requirements for hermetically sealing a large variety of medical devices, including pacemakers, batteries, and capacitors.

Initial trials were set up to discover weld parameters that would yield penetrations of approximately 0.20-0.25 mm. Table 1 is a summary of the data for each lens setup. As the data clearly shows, weld penetration increases with laser power, and at fixed powers, decreases with increasing feedrate as would be expected. During this portion of the study, it became evident that this laser's beam quality was sufficient to achieve keyhole like welds at average powers of only 250 W. Figure 2 is a plot of maximum penetration versus table feedrate for various power welds using the 150-mm focal length lens. Note the steep slope of the 250- and 350-W curves below feedrates of 50 ipm. These welds had distinctly different cross section profiles, more indicative of keyhole welds than simple conduction welds. Figure 3 is a cross section of a weld traverse completed using 250 W at 25 ipm. Figure 4 is a weld traverse completed at 250 W at 200-ipm feedrate. Note that the shoulder like feature has disappeared in the high feedrate weld. Similarly, Figure 5 is a plot of the penetration versus feedrate welds completed at various powers using the 200-mm lens. Again, note the abrupt change in slope at 50 ipm of the welds completed at 250 and 350 W. Figures 6 and 7 compare the cross section weld profiles of the 250-W traverses made at 25 and 50 ipm. Again, the keyhole like shoulder disappears at feedrates above 50 ipm.

Table 1. CW Nd:YAG Results

200-mm Lens Data - Bead-on-Plate Titanium (Ti 6Al-4V)					150-mm Lens Data - Bead-on-Plate Titanium (Ti 6Al-4V)				
Watts (Avg. Power)	Feedrate (ipm)	Width (mm)	Penetration (mm)	Ratio (width/pen)	Watts (Avg. Power)	Feedrate (ipm)	Width (mm)	Penetration (mm)	Ratio (Width/pen)
50	10	0.250	0.030	8.33	50	10	0.241	0.060	4.02
50	25	0.205	0.019	10.79	50	25	0.258	0.062	4.16
50	50	0.214	0.015	14.27	50	30	0.259	0.064	4.05
150	25	0.580	0.172	3.37	150	10	0.516	0.231	2.23
150	50	0.539	0.144	3.74	150	25	0.500	0.177	2.82
150	100	0.473	0.112	4.22	150	50	0.455	0.139	3.27
150	150	0.416	0.088	4.73	150	100	0.406	0.107	3.79
250	25	1.320	0.699	1.89	150	150	0.371	0.093	3.99
250	50	0.647	0.211	3.07	150	200	0.341	0.085	4.01
250	100	0.572	0.155	3.69	250	25	1.447	0.876	1.65
250	150	0.507	0.132	3.84	250	50	1.069	0.728	1.47
250	200	0.461	0.122	3.78	250	100	0.810	0.567	1.43
350	10	2.191	1.525	1.44	250	100	0.766	0.592	1.29
350	25	1.780	1.214	1.47	250	150	0.621	0.521	1.19
350	50	1.351	0.986	1.37	250	200	0.523	0.472	1.11
350	100	0.944	0.801	1.18	350	10	2.187	1.657	1.32
350	150	0.732	0.654	1.12	350	25	1.662	1.333	1.25
350	200	0.654	0.541	1.21	350	50	1.356	1.000	1.36
350	250	0.597	0.400	1.49	350	100	0.955	0.832	1.15
					350	150	0.781	0.737	1.06
					350	200	0.717	0.650	1.10

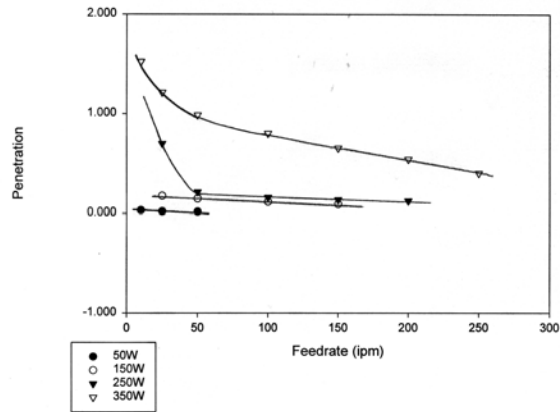


Figure 2. Plot of Penetration (in mm) versus Feedrate (ipm) for Bead-on-Plate CW Welds at Various Powers Using a 200-mm Focal Lens (Sample is 0.75-mm-thick Ti6Al4V.)

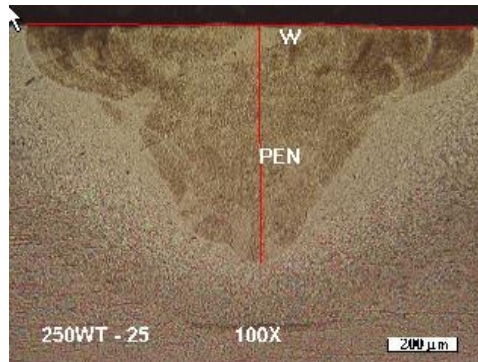


Figure 3. Cross Section of Bead-on-Plate Weld in Ti6Al4V (Laser conditions were 250-W CW, 200-mm lens at 25-ipm feedrate. Note area of deeper penetration and distinct shoulder indicative of keyhole-like penetration.)

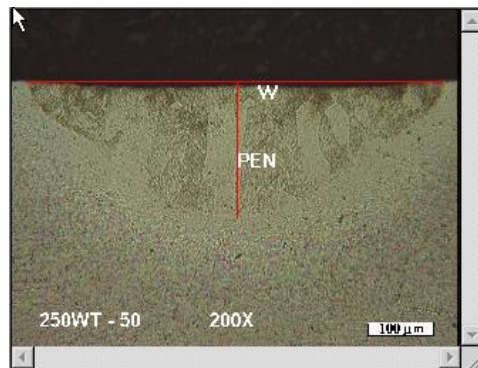


Figure 4. Cross Section of Bead-on-Plate Weld in Ti6Al4V (Laser conditions were 250-W CW, 200-mm lens at 50-ipm feedrate. Note area of deeper penetration does not have as distinct a shoulder region, indicative of standard conduction-like penetration.)

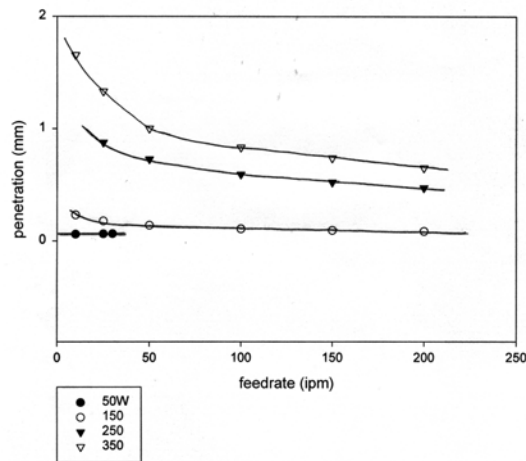


Figure 5. Plot of Weld Penetration versus Feedrate for Bead-on-Plate CW Welds at Various Powers using a 150-mm Focal Lens (Sample was 0.75-mm Ti6Al4V.)

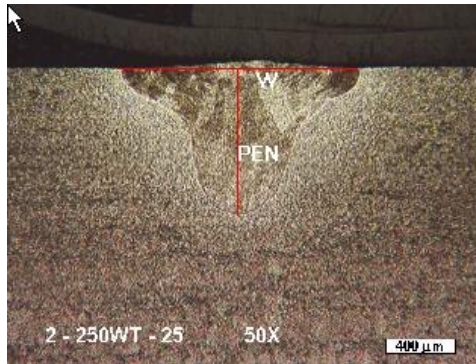


Figure 6. **Cross Section of Bead-on-Plate Weld in Ti6Al4V** (Laser conditions were 250-W CW, 150-mm lens at 25-ipm feedrate. Note area of deeper penetration and distinct shoulder indicative of keyhole-like penetration.)

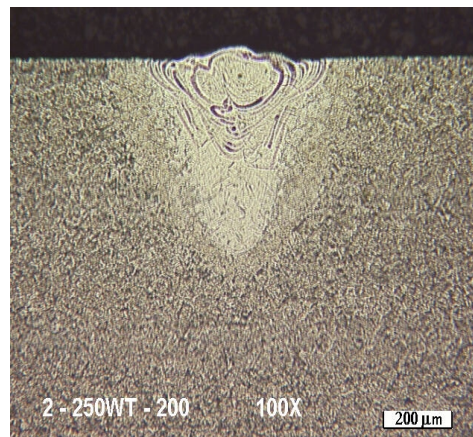


Figure 7. **Cross Section of Bead-on-Plate Weld in Ti6Al4V** (Laser conditions were 250-W CW, 150-mm lens at 200-ipm feedrate. Note area of deeper penetration does not have as distinct a shoulder region, indicative of standard conduction-like penetration.)

Using the initial data in Table 1 and subsequent trial runs, laser parameters for the temperature portion of the study were limited between 200-250 W. From this data it was determined that at powers of 200-250 W and feedrates of 25-200 ipm, the penetration range was 0.25 to 0.88 mm and typically between 0.20-0.25 mm. Temperature studies were then completed using both the 150- and 200-mm focal lens. In the first trials, the power was held constant at 200 W. In the second, both power and speed were varied for each lens setup.

Table 2 is the completed data set for the temperature phase of our study. The columns indicate the feedrate in inches per minute, the maximum recorded temperature in degrees Celsius, the elapsed time the thermocouple maintained a temperature above 300°C, and the power/feedrate ratio. The power/feedrate ratio is an indirect measure of

the thermal input, as it has both the power in watts and the time factor as measured by the feedrate contained within it. This was found to be a useful figure of merit in later calculations. The data table clearly shows that increasing feedrate lowers the both the maximum temperature and the time at which the part is at or above 300°C. Figure 8 is a plot of the maximum temperature versus feedrate for a constant power of 200 W and using the 150-mm lens. The plot indicates that at these laser parameters feedrates above approximately 75-ipm yield maximum temperatures below 300°C. Figure 9 is similar plot, this time using maximum temperature versus the power/speed ratio. This plot would indicate that power/speed ratios below 3.0 will keep the maximum temperature below the 300°C target. The data in Figure 9 has been curve fitted using standard regression techniques. The plotted line has an R² of 0.96 and an equation of:

$$F = 38.88 - 82.19x + 4.46x^2$$

where:

F = maximum temperature in degrees Celsius

x = power speed ratio (W/ipm)

Table 2. Maximum Temperature Data for 150-mm Lens Setup (Nominal Penetration 0.15-0.25 mm)

Lens (mm)	Power (W)	Feedrate (ipm)	Max. Temperature (°C)	Time to <300°C (sec)	Power/Speed Ratio
150	200	30	800	6.50	6.67
150	200	50	353	2.00	4.00
150	200	60	350	2.00	3.33
150	200	60	384	3.10	3.33
150	200	70	346	1.75	2.86
150	200	70	350	1.50	2.86
150	200	80	262	1.60	2.50
150	200	80	260	1.40	2.50
150	200	100	243	1.20	2.00

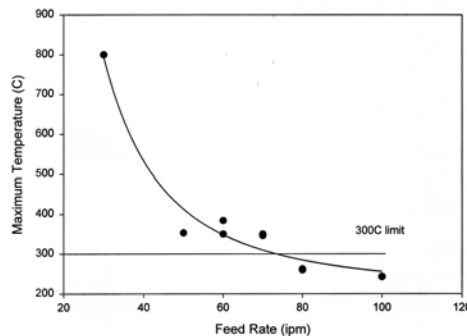


Figure 8. Plot of Maximum Temperature versus Feedrate for Bead-on-Plate CW Laser Welds using 200-W Fixed Power and a 150-mm Focal Lens (Sample was 0.75-mm Ti6Al4V with thermocouples ≈0.50 mm away from weld root.)

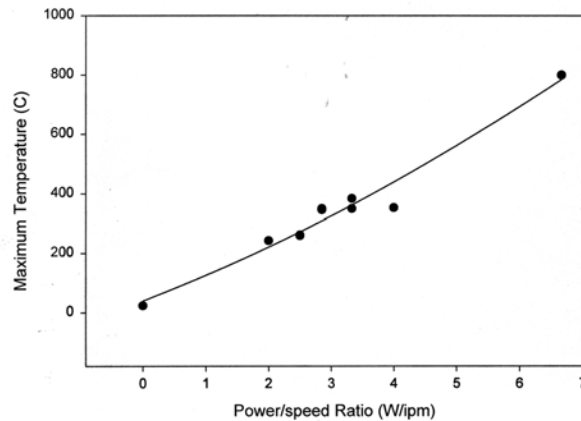


Figure 9. Plot of Maximum Temperature versus Power/Speed Ratio for 200-W Fixed Power Welds and 150-mm Lens (Power/speed ratios below 3.0 yield temperature extremes below the 300°C limit.)

Similarly, Table 3 is the data set for the trials completed using the 200-mm lens at various power settings up to 290 W. The feedrates were selected after inspection of pretrial cross sections. From these it was determined that feedrates above 80 ipm were required to achieve limited penetration at the higher powers. Again, the target penetration was held near 0.2 mm. Figure 10 is a plot of maximum temperature versus power/speed ratio for variable power and feedrate welds using the 200-mm lens. In this case, the plot indicates that the power speed ratio must be maintained below 2.2 to keep the weld temperatures below the 300°C limit. The data in Figure 10 were fitted using standard regression techniques yielding a fit of $R^2 = 0.987$ and an equation of:

$$F = 26.77 + 140.08x - 8.60x^2$$

where:

F = maximum temperature in degrees C
 x = power/speed ratio (W/ipm)

Table 3. Maximum Temperature Data for 200-mm Lens Setup

Weld No.	Lens (mm)	Power (W)	Feedrate (ipm)	Max. Temperature (°C)	Time to <150°C (sec)	Penetration (mm)	Width (mm)	Power/Speed Ratio
2	200	270	80	383	2.3	0.63	0.19	3.38
4	200	270	80	416	2.5	0.61	0.19	3.38
6	200	270	100	355	1.6	0.57	0.18	2.70
8	200	290	120	306	1.5	0.58	0.19	2.42
12	200	275	120	312	1.25	0.65	0.2	2.29
14	200	275	80	380	2.5	0.62	0.2	3.44
16	200	275	80	416	2.5	0.63	0.21	3.44
18	200	290	120	313	1.3	0.59	0.19	2.42
20	200	290	120	335	1.5	0.57	0.21	2.42
22	200	290	120	303	1.3	0.56	0.18	2.42
24	200	150	20	595	>10	0.66	0.2	7.50

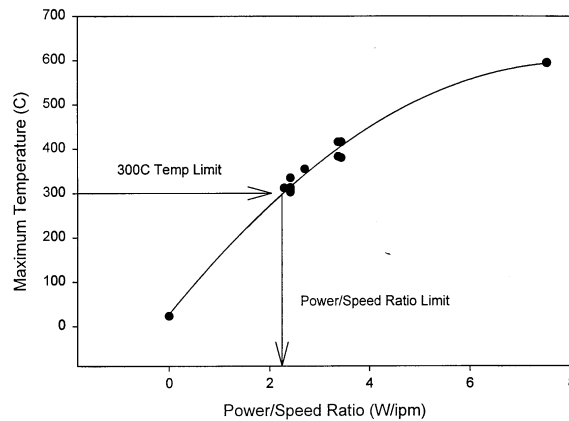


Figure 10. Plot of Maximum Temperature versus Power/Speed Ratio for Variable Power and Feedrate Welds Using 200-mm Lens (The 300°C temperature limit is predicted using power/speed ratios below approximately 2.2.)

Discussion

Other researchers have discussed the merits of pulsed Nd:YAG welding and measured temperature profiles in thin stainless steel packages [1]. In that work it was suggested that the time element of the process could be significant in the development of the maximum temperature [2]. This work has demonstrated that the temperature is a strong function of the feedrate in continuous wave welding and that keyhole like structures can be seen at lower feedrates [3,4]. Beam quality is also important, in that sufficient energy density in the spot can be achieved with higher beam quality systems. This allows the users to weld faster and/or at lower powers. For these types of welds in medical devices feedrates of 10-35ipm are more typical. The use of CW processing allows for faster feedrates to be used while achieving adequate penetration, low maximum temperatures, and good standoff distances due to longer focal length lens capability.

Conclusions

From this work we can conclude the following:

- The beam quality of this laser is sufficient to achieve keyhole like welds at powers of 250 W and feedrates below 50 ipm and using either 150- or 200-mm lens.
- The maximum temperature 0.50 mm from the weld root is a strong function of feedrate for CW processing.

- The maximum temperature is below 300°C using 200-W CW power and the 150-mm lens at feedrates above 75 ipm.
- The maximum temperature is below 300°C using the 200-mm lens when the power speed ratio is kept below 2.2.

References

1. Fuerschbach, P. W. and Hinkley, D. A. (1997). "Pulsed Nd:YAG Laser Welding of Cardiac Pacemaker Batteries with Reduced Heat Input," **Welding Journal Supplement**, 103-s to 109-s.
2. Gornyi, S. G., Lopota, V. A., Matyushin, I. V., Rudoi, I. G., and Soroka, A. M. (1988). "Comparison of the Efficiency of Heat Input in Laser Welding," **Svar. Proiz.** 8:31-32.
3. Okada, A. (1977). "Application of Melting Efficiency and its Problem," **J. Japan Welding Soc.** 46(2):53-61.
4. Fuerschbach, P. W. (1996). "Measurement and Prediction of Energy Transfer Efficiency in Laser Seam Welding," **Welding J.** 75(1):24-s to 34-s.